ORIGINAL ARTICLE

WILEY

Biological performance of a novel bovine hydroxyapatite in a guided bone regeneration model: A preclinical study in a mandibular defect in dogs

Bruno De Carvalho DDS, MS, PhD Fellow[1] | Emilie Dory DDS, MS[2] |
Caroline Trus DDS[2] | Justine Pirson DDS[2] | Loïc Germain DDS[2] |
Geoffrey Lecloux DDS, MS[1] | France Lambert DDS, MS, PhD[1] |
Eric Rompen DDS, MS, PhD[2]

[1]Department of Periodontology, Oro-Dental and Implant Surgery, Dental Biomaterial Research Unit, Liège, Belgium

[2]Wishbone SA, Liège, Belgium

Correspondence
France Lambert, Department of Periodontology, Oro-Dental and Implant Surgery, Dental Biomaterial Research Unit, Avenue de l'Hôpital 1, 4000 Liège, Belgium.
Email: france.lambert@chuliege.be

Abstract

Objectives: This preclinical model study aims to evaluate the performance and safety of a novel hydroxyapatite biomaterial (Wishbone Hydroxyapatite, WHA) on guided bone regeneration compared to a commercially available deproteinized bovine bone mineral (Bio-Oss, BO).

Material and Methods: Twenty-four beagle dogs were allocated to three timepoint cohorts (4, 12, and 26 weeks) of eight animals each. In all animals, four critical-sized, independent wall mandibular defects were created (32 defects/cohort). Each animal received all four treatments, allocated randomly to separated defects: WHA + collagen membrane (M), BO + M, no treatment (Sham, Sh), and Sh + M. At each timepoint, the specimens were harvested for histologic and histomorphometric analyses to determine the newly formed bone and osteoconductivity.

Results: At 4 weeks, bone regeneration was significantly higher for WHA + M (46.8%) when compared to BO + M (21.4%), Sh (15.1%), and Sh + M (23.1%) ($p < 0.05$); at 12 and 26 weeks, regeneration was similar for WHA and BO. Bone-to-material contact increased over time similarly for WHA + M and BO + M. From a safety point of view, inflammation attributed to WHA + M or BO + M was minimal; necrosis or fatty infiltrate was absent.

Conclusions: WHA + M resulted in higher bone regeneration rate than BO + M at 4 weeks. Both BO + M and WHA + M were more efficient than both Sh groups at all timepoints. Safety and biocompatibility of WHA was favorable and comparable to that of BO.

Summary Box

What is known?

- Several types of natural hydroxyapatite of bovine origin are available for the reconstruction of alveolar bone defects. Nevertheless, their biological performance is highly dependent of their own physicochemical characteristics and manufacturing processes.

What this study adds?

- The present study evaluates the biocompatibility and biological performance of a novel bovine hydroxyapatite with different manufacturing processes when compared to a control biomaterial, demonstrating how different physicochemical compositions can have an impact in regenerative outcomes.

1 | INTRODUCTION

The use of dental implants to replace missing teeth has increased over the last decades.[1] A common problem encountered in the dental implant rehabilitation is the lack of sufficient bone volume and alveolar bone augmentation procedures are often necessary prior to or simultaneously to implant placement.[2–7]

Autogenous bone has long been regarded as the gold standard for bone augmentation procedures[8–11] as the material is histocompatible and possesses osteoinductive, osteoconductive, and osteogenic properties. However, its use is limited by availability, increased morbidity and scarring at the donor site, and high resorption rates.[8,12–15] Guided bone regeneration using biomaterials as bone fillers represent an alternative used in oral surgery, implantology and periodontology as they allow bone ingrowth and osteoconductive structural guidance.[3,16,17] Currently, several types of bone graft substitute biomaterials are available, each with their own advantages and disadvantages.[7,17,18] Natural and synthetic calcium phosphate bone graft substitutes such as hydroxyapatite (HA) and tricalcium phosphate are the most widely used biomaterials for alveolar bone regeneration.[15,19,20] Natural HA of bovine origin has some advantages over synthetic scaffolds because of its physicochemical properties such as surface structure, morphology and microporosities that closely resemble those of natural bone, if not manufactured at high sintering temperature.[21–23] Indeed, high sintering temperature of bovine HA have an influence of the surface topography and therefore on the osteoconductive potential.[24] Additionally, the slowly resorbable feature of natural bovine HA materials is of great interest in the field of dentistry, as one of the goals of bone regenerative treatments is to maintain the volume over time and to allow a denser composite regenerated bone tissue.[16,25]

Several natural HA biomaterials are available; among these, DBBM has been distinguished itself as the most documented natural HA bone substitute of bovine origin in regenerative dentistry for over 30 years.[26] Recently, a novel HA bone substitute has been granted marketing approval by the United States Food and Drug Administration[27] in which the complete elimination of the organic residues is performed under subcritical conditions and a continuous flow of a basic solution following the patented extraction method (WO 2015/049336 A1).[28] Both biomaterials are xenograft biomaterials composed of HA of bovine origin, intended for the filling, augmentation, or reconstruction of alveolar bone defects.[27,29] The aim of this study was to evaluate the biocompatibility and biological performance (new bone formation and osteoconductivity) of novel HA bone substitute on guided bone regeneration in comparison with a control biomaterial as it is considered as the gold standard of xenogeneic materials in regenerative dentistry.

2 | MATERIALS AND METHODS

2.1 | Biomaterials characterization

Two xenografts composed of HA of bovine origin were used in the present study: Wishbone Hydroxyapatite (WHA, Wishbone SA, Liège, Belgium) and Bio-Oss (BO, Geistlich Pharma AG, Wolhusen, Switzerland). Physicochemical characterization was performed in both xenografts in terms of Scanning Electro Microcopy (SEM) x-ray diffraction (XRD), specific surface area (SSA), remnant organic compounds, elemental concentration, and volumetric porosity.

SEM provided the observation of the micro-organization of the surface morphology at magnification 500× and 1000× (ESEM-FEG XL30 (Philips Electron Optics, Hillsboro, OR, USA)). XRD identified the phase composition, crystallite size and crystallinity ratio present in the samples and was acquired by means of Rietveld refinement, using the crystal structure model for HA of PDF card 01-076-0694. The SSA of each product was measured by N_2 adsorption according to the Brunauer–Emmett–Teller (BET) method analyzed on the TriStar 3000 equipment. For the analysis of the remnant of organic compounds, three samples of each material were heated successively to three different temperature stages in a furnace, resulting in thermal oxidation and conversion of carbon into gaseous CO_2 which is measured by means of an infrared detector. A temperature measurement of total carbon was applied to quantify both the total organic carbon released up to $400°C$. Elemental composition of Ca, P, Mg, and Na were calculated in which three samples of each material were digested in
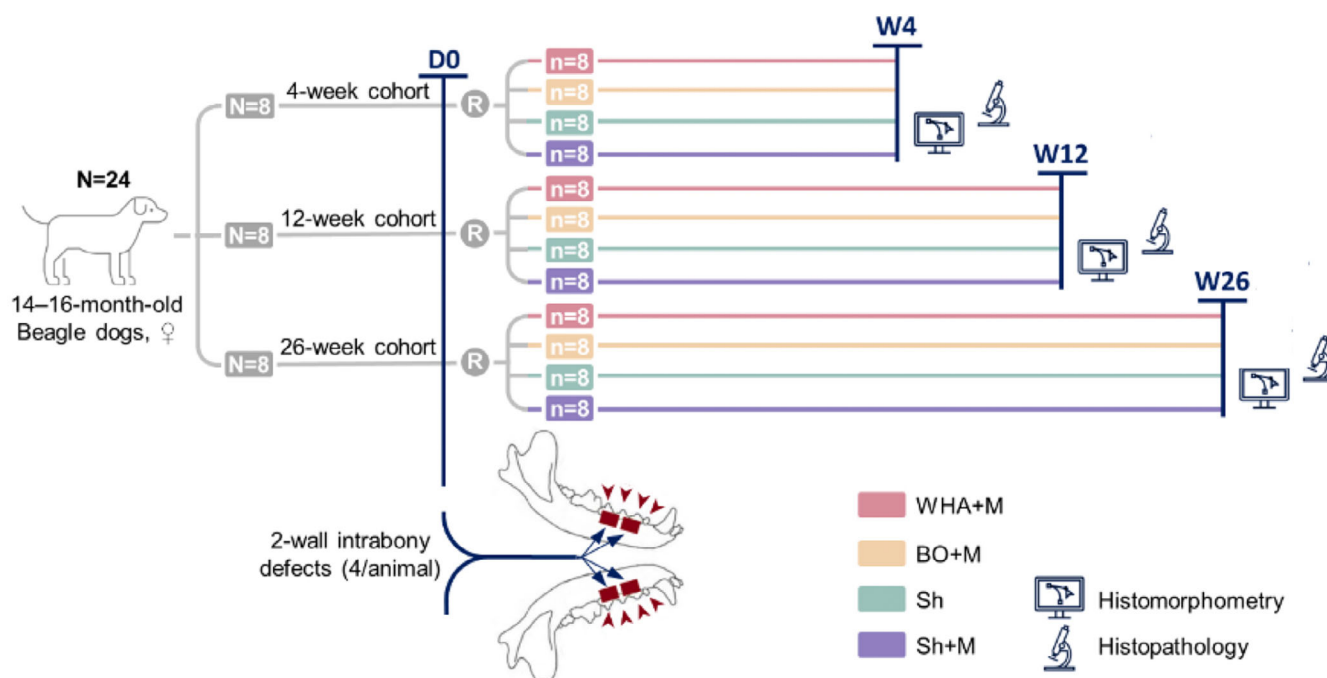
FIGURE 1 Study design: N, number of dogs/specimens; D, day; R, randomization; W, week; n, number of defects. The red arrows indicate extracted teeth (premolar [PM]1–PM4); red rectangles denote the bone defects created.

concentrated HNO_3 and diluted 1:100 in a dilute acidic solution for trace/impurity element determination, and 1:1000 for Ca and P determination. Calibration solutions are prepared by diluting certified multi- and single-element standard solutions. Element concentrations in the solutions are quantified on an Agilent 7700x ICP-MS and evaluated using Agilent "Masshunter" software. To determine volumetric porosity 1.5 g granules were filled into a container and tapped 1000 times under specified conditions on a pneumatic device. Subsequently, the granules protruding a defined upper edge of the container are scraped off and the mass of the granules inside the container is determined on an analytical scale. Finally, the tapped density is obtained by division of the mass by the volume of the container ($1.4 \ cm^3$).

2.2 | Experimental animals

Twenty-four 14–16-month-old female Beagle dogs (Marshall Bioresources, New York, USA) weighing ~6 to 8 kg were allocated to three timepoint cohorts (4, 12, and 26 weeks) of eight animals each. The canine model was chosen due to its bone density, mechanical properties, morphological structure and healing capacity similar to the human bone.[30]

2.3 | Ethics statement

The study protocol was reviewed and approved by the Committee Review of the testing facility, Charles River Laboratories Montreal ULC, Boisbriand, Canada under the ethical approval number 2889-416G. The review ensured compliance with appropriate

regulations. The testing facility is accredited by the Association for Assessment and Accreditation of Laboratory Animal Care and the Canadian Council on Animal Care. The reporting of this preclinical study follows the recommendations contained in the Animal Research Reporting of In Vivo Experiments (ARRIVE) guidelines.

2.4 | Study design

For each animal, four independent wall defects were created (two per hemimandible), resulting in a total of 32 defects for each timepoint (4, 12, and 26 weeks) (Figure 1). Each animal received all four treatments. One material-filled defect (test: WHA + membrane [M] or control: BO + M) and one sham control defect with or without a collagen membrane (sham [Sh] or Sh + M) were randomly allocated to each side of the mandible. Randomization was carried out based on a predetermined allocation plan.

2.5 | Surgical procedure

Tooth extraction, defect creation and regenerative procedures were performed in a single step under general anesthesia. Four premolars were extracted on each side of the mandible, and two independent critical-sized wall defects of 10.0 mm (mesio-distally), 8.0 mm (vertically), 6.0 mm (bucco-lingually) were created on each side by totally removing the buccal alveolar plate and partially the lingual one by means of a bone saw disc (Figure 2). No template was used to perform the critical-sized defects. The surgeons calculated the available space
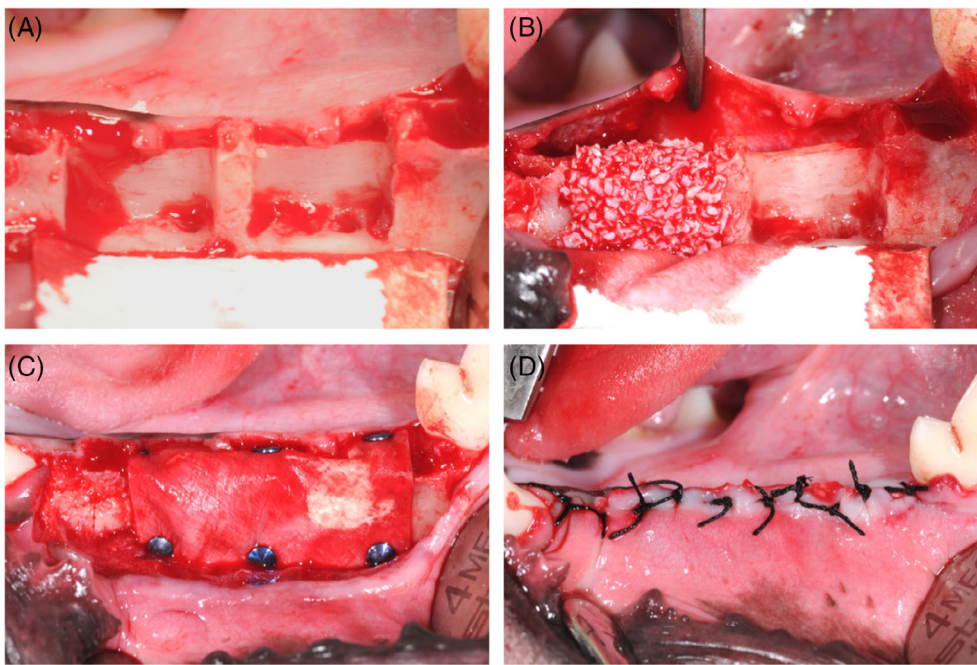
FIGURE 2 Critical bone defects of each hemimandible. (A) Critical bone defects perform in a hemimandible. (B) BO and Sh + M allocation. (C) Collagen membrane placement anchored with pins. (D) Flap closure.
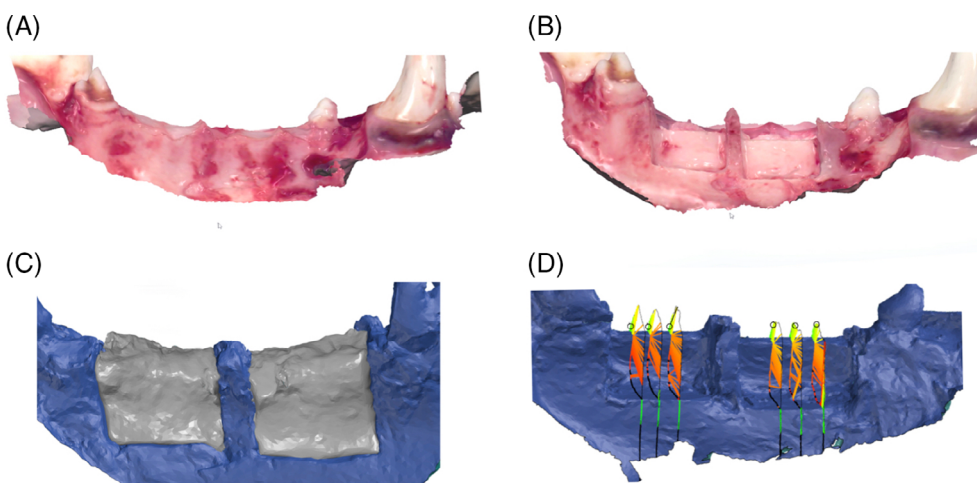

FIGURE 3 (A) Baseline IOS from the edentulous crest after dental extraction; (B) IOS of the critical bone defects; (C) superimposition of the baseline and critical bone defects IOS's; (D) definition of the area for the histological sections for histomorphometry and histopathology.

of the crest after extraction by means of a periodontal probe, assuring the protocolized measurements of the critical-sized defects as they were making the defect cut. For anatomical reasons, back and frontal defects in each hemimandible slightly differed in size, but this had no impact on the results generated in the study since the attribution of the defects to a control or test group was randomized.

An intraoral scan (IOS) imaging of the edentulous area and of the empty defect was performed to have the baseline dimensions, and then the defect was randomly allocated to one of the four groups. In the groups allocated for a regenerative procedure (WHA and BO), the defect was filled with the biomaterials and a resorbable collagen membrane (Creos Xenoprotect, Nobel Biocare, Switzerland) stabilized with anchor pins (Bone Tac Screw 5.0 mm GDT implants, Israel). The sham defects in control groups were left empty and one was covered with the collagen membrane also fixed with anchor pins.

The muco-periosteal flaps were sutured with nonabsorbable sutures (Seraflex 4/0, Serag Wiessner). To prevent postoperative infection, animals received a prophylactic antibiotic (Cefazolin 25 mg/kg, IV) during the preparation procedures. In the postoperative period, the animals received Carprofen (Rimadyl) 3–5 mg/kg PO (per os) to control postoperative pain and inflammation. Following surgical procedures, the animals were housed in individual cages. Housing was modified to prevent the dogs from chewing on housing material/devices and possibly damage the surgical site.

2.6 | IOS and defect wall homogeneity evaluation

For each defect created, an optical impression from a buccal, coronal, and lingual view (from the first remaining canine tooth to the first remaining molar tooth, both included) was taken using an intraoral scanner (Trios 3®, 3Shape, Copenhagen, Denmark). Each hemimandible was scanned before defect creation and after defect creation (Figure 3A,B).
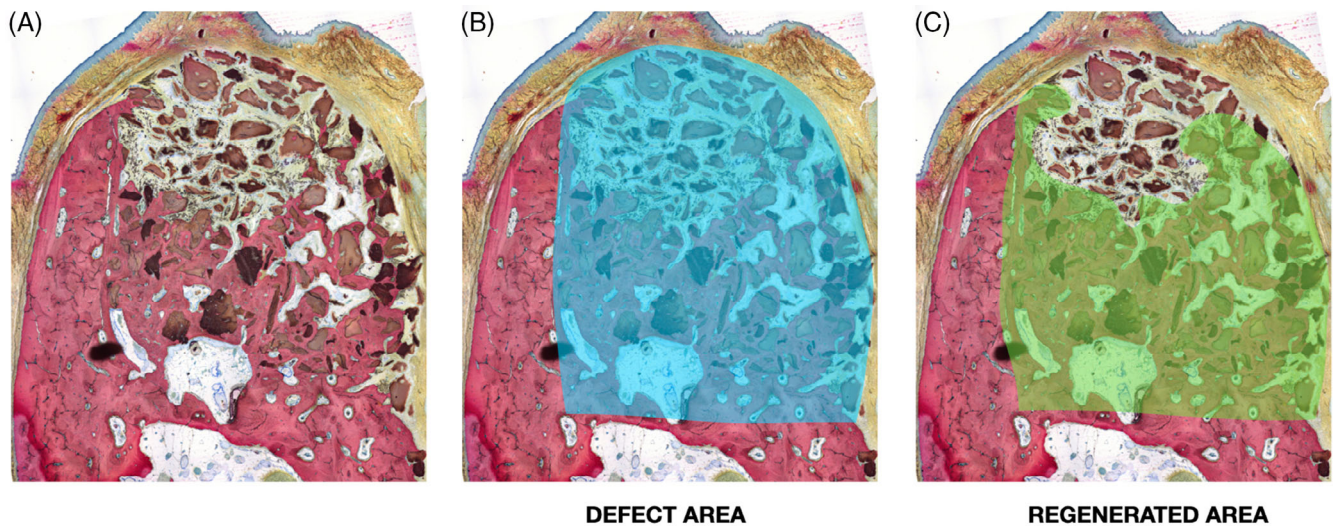
FIGURE 4 Tracing of ROI1 and ROI2 for histomorphometric analyses. (A) WHA + M at 12 weeks; (B) defect area highlighted in blue (ROI1); (C) regenerated area highlighted in green (ROI2).

IOS scans were used to consistently select bone areas for histological processing and analysis. The scans taken before and after defect creation were superimposed based on the position of the remaining canine and first molar teeth (Figure 3C). The exact size and volume of the defects were calculated using surface-based analysis software (GOM Inspect Professional). The cross-sectional area of the mandibular bone that was present in the scan taken before defect creation but absent in the scan taken after defect creation was used to define the original defect area, named as region of interest (ROI) 1.

2.7 | Histology processing

Nondecalcified histology of the retrieved specimens was performed. To match the intraoral scanning data with the specimen, the distance from the center of the bone ridge in between the defects to the region of interest was used to match the slide position. Samples were fixed in 10% neutral-buffered formalin solution, followed by dehydration in a series of graded ethanol solutions, and finally embedded in methyl-metacrylate resin. For each defect, six sections (20–40 μm thick) were performed in each specimen (two sections located at the center of the defect, two other sections located in the mesial end and two others in the distal end of each defect) (Figure 3D). From these sections, three sections were stained with hematoxylin and eosin for histopathology analysis, and three other were stained with Stevenel's blue for both histomorphometry and histopathology analysis.

2.8 | Histomorphometry evaluation

All sections from all bone defects were digitally captured (Clemex Vision Lite Software) to obtain whole-section images by microscope with a 10× objective (Nikon Eclipse LV100ND, Tokyo, Japan). To evaluate the extent of bone regeneration, histomorphometric measurements were performed on selected scans using Image-Pro Premier 9.2 software (© Media Cybernetics, Inc., USA). Depending on the structure to analyze, both manual tracing or automatically measured based on the color and color intensity differences were used.

The *defect area* (ROI1) was defined precisely for each defect based on IOS measurements. The regenerated area (ROI2) was defined by the surface of the original defect colonized by newly formed bone (Figure 4). For the histomorphometric, analyses were made based on the mean of three sections per defect and the following variables were collected:

- *Defect area*: defined as the total area of the defect (Region of Interest, ROI1) (Figure 4B).
- The *regenerated area* (ROI2), defined as the portion of the defect area (ROI1) colonized with newly formed bone (Figure 4C).
- The percentage of newly formed bone (B), biomaterial (M), and soft tissue (S) in the defect area (ROI1).
- The percentage of *bone-to-material contact (BMC)* characterizing the osteoconductivity and defined as the percentage of the biomaterial perimeter in contact with newly formed bone within the regenerated area (ROI2).

2.9 | Descriptive and histopathological evaluation

Descriptive analyses as well as safety and biocompatibility semi-quantitative analyses of the implanted materials were evaluated on both Stevenel's blue and Hematoxylin–Eosin stained histology sections of the bone defects by a single pathologist. Sections were analyzed and graded according to the presence of different cell types and tissue responses, including necrosis, fibrosis, and

neovascularization (Table A1). An irritancy scoring system adapted from the ISO 10993-6 Annex E[31] was used to compare the biocompatibility of the different study materials. Average irritancy scores for each group were calculated at each timepoint. Based on the difference between the irritancy score of WHA + M and that of the comparator treatments, WHA + M was to be considered as nonirritant at ≤2.9 points difference, a slight irritant at 3.0–8.9 points difference, a moderate irritant at 9.0–15.0 points difference, and a severe irritant at >15 points difference.

2.10 | Statistics analyses

2.10.1 | Sample size calculation

The sample size was calculated using the software Gpower 3.1.[32] Assuming an effect size of 0.6, an alpha error of 0.004 (corrected for multiple comparisons), and a power of 95%, the obtained total sample size was 95. Thus, 24 animals received one of each four conditions and were randomly divided into three cohorts for the three observation periods (4, 12, and 26 weeks), giving a total sample size of 96.

2.10.2 | Statistical tests

Means and standard derivations were reported for quantitative outcomes. A mixed effect model with individual animal as a random effect and treatment, location, time and the interaction between week and treatment was used to compare WHA against BO and sham controls. Analysis of variance was performed using SAS 9.4 (SAS Institute Inc., NC, USA) to identify the differences of least square means between the treatments. The Tukey–Kramer method of multiple testing correction was used.

3 | RESULTS

3.1 | Study design

All study animals survived until the scheduled sacrifice. Their body weight remained stable over the course of the study and was consistent with the experimental model. IOS measurements demonstrated that the size of the defects, as well as the defect walls, were homogenous. For anatomical reasons, back and front defects slightly differed in size, but this had no impact on the results generated in the study, since attribution of the defects to a group was randomized.

At 12-weeks, one animal had notably higher inflammation associated with both WHA and BO defects, as well as inflammation associated with the sham defects. In addition, there was significant migration of particles out of one of the WHA defects in another animal. To present the effect of implanted biomaterials on bone regeneration more accurately, results from these five outlier defects were excluded from the analysis; therefore, week 12 data are based on six defects for the WHA group and on seven defects for the BO, Sh and Sh + M groups.

3.2 | Physicochemical characterization

The XRD analysis demonstrate that the crystallographic phase composition of all WHA and BO samples consists in 100% of hydroxyapatite with no secondary phase (limit of detection ≤ 0.88 wt%). Hence, regarding phase composition, the WHA and BO products are equivalent. The crystal size is lower in BO compared to WHA samples which is a parameter influenced by the heat treatment at high temperatures increasing the crystal size and decreasing solubility of hydroxyapatite bone substitutes. Specific surface area analysis showed that the mean for WHA and BO samples are 16 m^2/g and 81.7 m^2/g, respectively. These results demonstrate that WHA presents a moderate specific surface area while BO presents a high specific surface. The results of organic carbon released up to 400°C showed that a low amount, if any, of organic residues are found in both WHA and BO products given that the values for the 6 samples are below or equal to 0.1 wt% where <0.1 designates the limit of determination. Volumetric porosity analysis reveals that WHA and BO products have a similar porosity. The results of the above-mentioned characterizations are presented in Table 1. Regarding the elemental composition (Table 2), the results obtained for the six samples show that Ca, P, Mg, and Na concentrations in WHA and Bio-Oss products are similar.

3.3 | SEM characterization

The micro-organization of the surface was observed at magnification 500× and 1000×. SEM images of WHA and BO are displayed in Figure 5. Fibril-like structures are observed in both materials with a periodical organization of the collagen fibrils and a close contact between collagen and hydroxyapatite within the bone matrix. The observation of this micro-organization demonstrates that WHA like Bio-Oss, retrieves the main characteristics of bone hydroxyapatite with its microporous and rough surface.

3.4 | Quantitative histomorphometric analysis

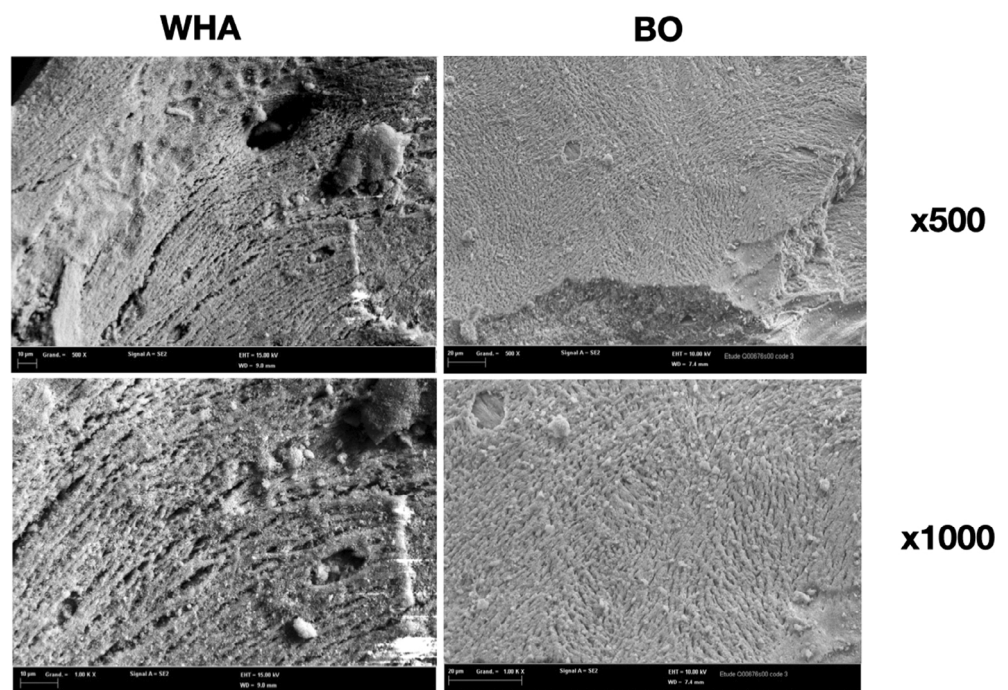### 3.4.1 | % Regenerated area (ROI2/ROI1) (4, 12, and 26 weeks)

At 4 weeks, the percentage of regeneration in the defect area ROI2 was significantly higher in the WHA group (46.8%) compared to the BO group (21.4%) and the sham control groups (Sh (15.1%), Sh + M (23.1%)) ($p < 0.050$) (Figure 6). At 12 weeks, bone regeneration was significantly higher in both the WHA (70.7%) and BO (73.9%) compared to the sham control groups (respectively, Sh (17.6%), Sh + M (33.2%)) with no significant differences between the two biomaterial groups. At 26 weeks, a higher percentage of regeneration was observed in the

TABLE 1 Biomaterials characterization: Organic content, phase composition, crystal size, porosity, and specific surface area.

Biomaterial	Organic content (wt%)	Phase composition (% of HA)	Crystal size (nm)	Porosity (%)	Specific surface area (m^2/g)
WHA	<0.1	100	54.4	82.3	16.0
BO	0.1	100	15.5	83.6	81.7

TABLE 2 Elemental composition analysis for Ca, P, Mg, and Na.

Biomaterial	Ca (%w/w)	P (%w/w)	Mg (%w/w)	Na (%w/w)
WHA	38.9	18.1	0.64	0.38
BO	37.3	17.0	0.59	0.46

FIGURE 5 Scanning electronic micrographs (SEM) of the studied biomaterials at different magnifications: WHA and BO with 500× and 1000× magnification. WHA and Bio-Oss, presenting both microporous and rough surface.

WHA + M (59.9%) compared to both sham control groups as well as in the BO + M (54.3%) group compared to the Sh group.

3.4.2 | Newly formed bone + biomaterial within defect area (ROI1) (4, 12, and 26 weeks)

At 4 weeks, the percentage of newly formed bone was significantly higher in the WHA group (9.5%) compared to the BO group (5.8%) (Figure 7). The BO group (5.8%) displayed less newly formed bone than the two shams with a significant difference with the Sh + M (9.3%). At 12 weeks, the percentage of newly formed bone was no significantly different in the two biomaterial groups (WHA: 23.4%, BO: 30.9%). Moreover, the Sh + M (21.9%) presented significantly more newly formed bone than the Sh without membrane. At 26 weeks, the percentage of newly formed bone was stable compared to the 12 weeks cohort and no significant differences are observed in between the biomaterial groups (WHA: 23.8%, BO: 25.8%).

The percentage of biomaterial presented no significant differences in between implanted groups in the three timepoints (Figure 7). However, a decrease was observed at 26 weeks in the BO groups.

3.5 | BMC (ROI2) (4, 12, and 26 weeks)

The bone-to-material contact within regenerated area ROI2 increased over the three time points at similar rates in the WHA and the BO groups with no significant differences between the two groups (Figure 8).

3.6 | Descriptive, safety, and biocompatibility analyses

After 4, 12, and 26 weeks, newly formed bone was found in the defect of all samples. Macroscopically (Figure 9), in both sham groups,
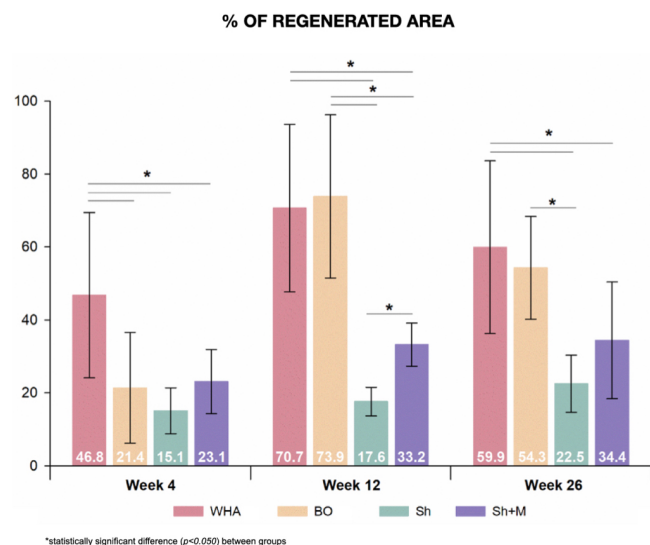
% OF REGENERATED AREA

*statistically significant difference (p<0.050) between groups

FIGURE 6 Evolution of defect area regeneration over time. Week 4 is marked by significant differences in between WHA + M and all other groups ($p < 0.05$). At week 12 both WHA + M and BO + M present significant differences in between both Sh and Sh + M groups. Week 26 WHA + M maintains its significant differences in between Sh and Sh + M. BO + M show significant differences only to Sh group.

woven bone was observed at 4 weeks while at 12 and 26 weeks a more cortical lamellar bone was observed with a noticeable lack of buccal bone volume. In the biomaterial groups, woven bone was predominately present in the WHA group at 4 weeks when compared to BO, nevertheless, at 12 and 26 weeks both groups present more mature bone in between the particles in the regenerated area.

Microscopically (Figure 10), in the implanted groups (WHA and BO) at 4 weeks the newly formed bone was immature and with thick trabeculae. At 12 and 26 weeks, the newly formed bone was in close contact with the biomaterial particles in both groups and bridged the particles together. At 12 weeks, the newly formed bone was still immature compared to the bone at 26 weeks displaying a lamellar organization. Some chains of osteoblasts are also observed close to the newly formed bone as well as some blood vessels, with no visible differences between the groups.

Histopathological examination revealed minimal inflammation within the defect area across all three timepoints and in all four groups. At all three timepoints, there was minimal inflammation attributed to either WHA + M or BO + M, and no necrosis or fatty infiltrate was observed. WHA + M was considered a nonirritant compared to BO + M at all three timepoints, and a slight irritant compared to Sh and Sh + M at 12 and 26 weeks (Table 3). Week 12 data did not include the results from one animal that had a more severe inflammatory response in all defects compared to the other animals in the same cohort.

The higher irritancy scores in the WHA + M group at weeks 12 and 26 were partly due to higher scores for fibrosis and neovascularization (data not shown). In the WHA + M group, fibrosis was

observed under the membrane, within the defect area, and surrounded the WHA granules outside of the area of new bone formation; conversely, for the Sh and Sh + M groups, the periosteum/membrane generally directly (or almost directly) overlaid the area of new bone formation that was associated with little fibrosis.

In all groups, there was low amount of neovascularization and fibrosis over time; in the WHA + M and BO + M groups, it was due to the growing area of new bone and marrow that replaced the fibrous tissue surrounding the granules, while in the sham control groups, it was largely due to the healing process and further collapse of the membrane/periosteum over the growing area of new bone.

4 | DISCUSSION

The present study was able to assess the biocompatibility and biological performance of WHA for guided bone regeneration in comparison to a widely used DBBM (BO), to the absence of filling biomaterial with and without a collagen membrane in a canine mandibular critical-sized bone defect model. Both biomaterials promoted bone regeneration in a similar extent and were not suspected to cause any predisposing factors to the pathogenesis of any of the observed clinical signs, revealing an excellent safety profile. Nevertheless, at 4 weeks, almost 50% of the defects were regenerated in the WHA group while only 21% of regeneration was found in the BO group, suggesting a different regenerative kinetic and higher osteoconductive properties for WHA. One hypothesis for this regenerative behavior at 4 week time point could be the different specific surface area (SSA) between the materials (BO 79.7 m^2/g[33] vs WHA 16.0 m^2/g according to the manufacturer). Specific surface area has been often mentioned in the literature as a significant parameter for bone regeneration.[34–36] However, these different SSA values, translates in different micro and nanoporosities between the materials. The higher micro and nanoporosities of BO might increase Ca^{2+} uptake from the extracellular fluids, decreasing its availability in the extracellular environment. WHA having less micro and nanoporosities, may allow more extracellular Ca^{2+} availability enhancing the effect of BMP-2 on Osteocalcin, Runx2 and Osterix expression, promoting faster bone regeneration in vivo.[37,38] At 4 weeks, BO showed significantly less % of newly formed bone of when compared to Sh + M, This results are in accordance to the literature[39,40] where in early stages of healing BO can delay the healing when compared to nongrafted sites.

The crystal size is lower for BO samples compared to WHA samples. It is indeed known that heating treatments at high temperatures increase the crystal size and decrease the solubility of hydroxyapatite bone substitutes, which is a parameter that might only impact the performances.[41] However, as demonstrated by our group similar performances for the unsintered hydroxyapatite and the hydroxyapatite sintered at mid-range temperature (820°C) proving that a crystal size up to 120 nm has no impact on the performances of hydroxyapatite from bovine origin. Based on that, the higher crystal size of WHA compared to BO has no impact on its performances.
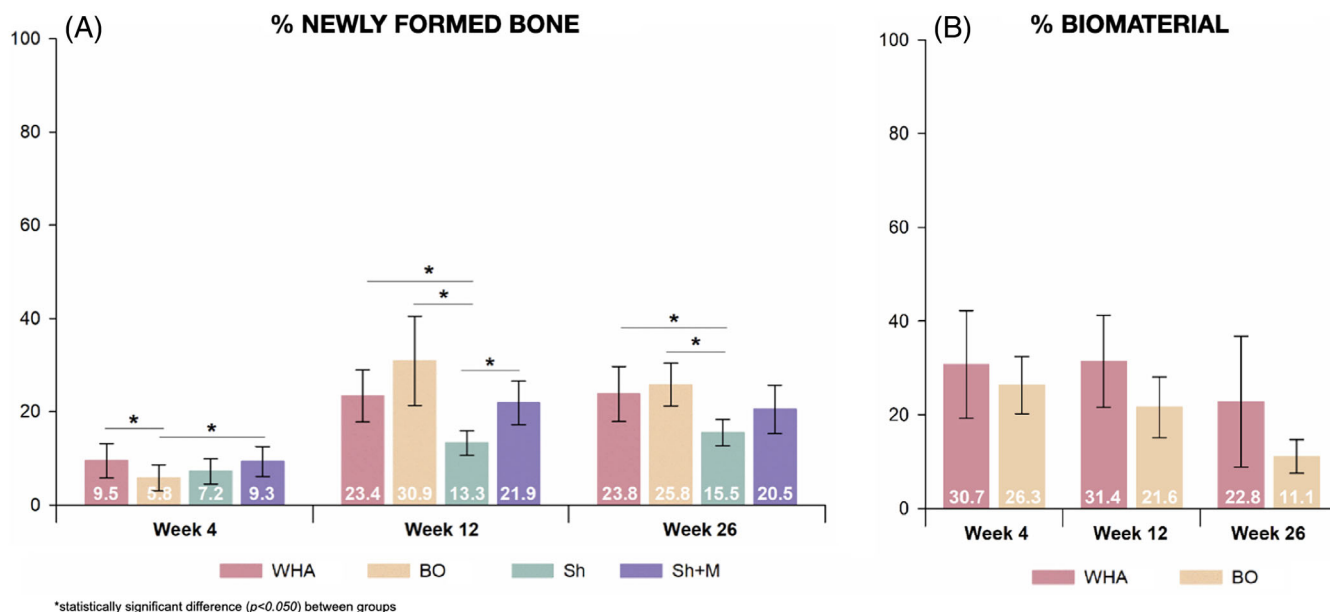
FIGURE 7 (A) Evolution of % newly formed bone overtime in all groups. At week 4 statistically significant differences in between WHA + B and BO + M ($p < 0.05$) and between Sh + M and BO + M ($p < 0.05$. At week 12 statistically significant differences in both WHA + M and BO + M when compared to Sh ($p < 0.05$) and significant differences in between Sh + M and Sh. At week 26 significant differences and maintained in both WHA + M and BO + M when compared to Sh ($p < 0.05$). (B) % of biomaterial over time within ROI1 in WHA + M and BO + M with no statistically significant differences in between groups during the 3 time points.

TABLE 3 Average histopathological irritancy scoring.

	Treatments			
Timepoint	WHA + M	BO + M	Sh	Sh + M
4 weeks	11.0	17.1	14.6	14.3
12 weeks	9.9	8.4	2.7	5.0
26 weeks	9.6	7.1	1.6	4.3

Abbreviations: BO, control hydroxyapatite; M, membrane; Sh, sham; WHA, test hydroxyapatite.

Moreover, bone-to-material-contact (BMC) was similar in the WHA and BO groups and appeared to increase over time at a similar rate. This parameter allows the evaluation of the osteointegration and osteoconductive behavior of the bone substitutes and can be correlated to surface topography and / or to sintering temperatures used in the manufacturing process, as suggested in our previous data. The manufacturing process of both bone fillers used in the present study allow to preserve a certain surface roughness, favoring cell colonization, osteoconductivity and better bone regeneration.[15,24] High osteoconductive properties are relevant from a regenerative point of view since a tight network between bone and biomaterial play an important role in implant primary stability and implant survival rates.[15,42,43]

From week 12 onwards, the use of either bone filler materials resulted in increased bone regeneration when compared to Sh and Sh + M group. This shows that the use of a bone filler material under collagen membrane enhances bone regeneration supporting

mineralization process and remodeling, when compared to the use of a membrane alone or no membrane as described in several studies.[44–46] The key role of barrier membranes for GBR procedures
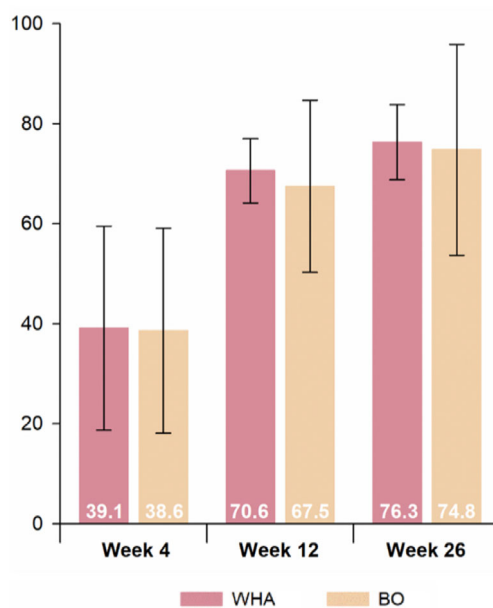

FIGURE 8 Evolution of bone-to-material contact within ROI2 in the groups WHA + M and BO + M during the 3 time points. No statistically significant differences in between groups.
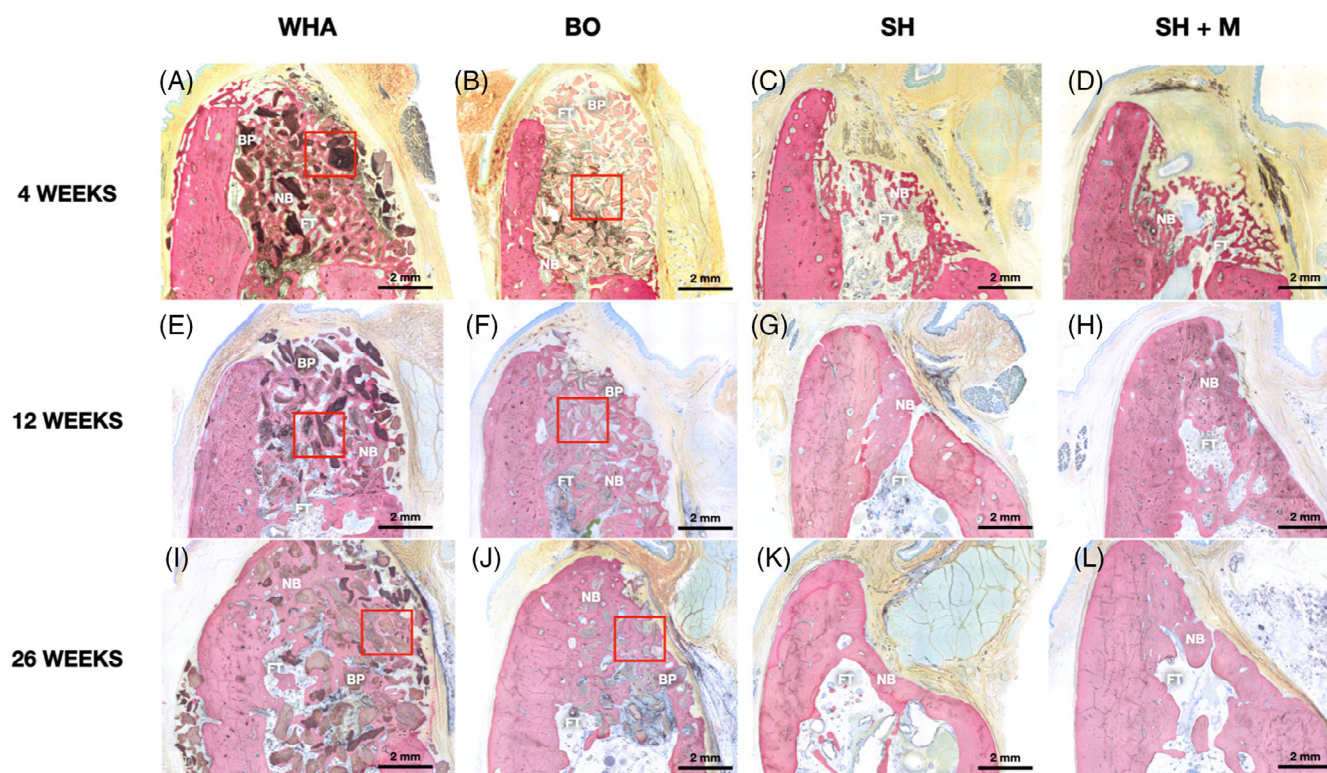
FIGURE 9 Descriptive histology at 4, 12, and 26 weeks. BP, bone particle; FT, fibrous connective tissue; NB, newly formed bone. The red squares correspond to the magnification areas presented in Figure 10.

in preventing the ingress of cells form the surrounding soft tissues, favoring osteoprogenitor cells for new bone formation is well described on the literature.[47,48] The results of the Sh + M group in the present study clearly show the role of the barrier membrane in the % of new bone formation, since this group performs significantly better than BO + M at 4 weeks, significantly better than Sh group at 12 weeks and presented at 26 weeks equivalent results than WHA + M and BO + M.

At 26 weeks, the % of regenerated area in the biomaterial groups decreases from the previous timepoint at 12 weeks. This can be explained by a residual remodeling of the crest, resorption of the biomaterial at 26 weeks[49] and the fact that the region of interest that was used to calculate this variable was the ROI1, corresponding to the baseline ROI before defect creation.

Volume stability over time also represents a crucial factor for the success of bone regeneration procedures and it is affected by the biodegradation rate of biomaterials[37,50] which depends on various factors like microporosities, chemical structure, crystallinity and local biological environment.[51,52] In the present study, it was not possible to assess the biodegradation rate of the studied biomaterials. Nevertheless, at 26 weeks WHA group presented a % of biomaterial with no significant differences when compared to BO group described in the literature as a biomaterial with high dimensional maintenance,[25,39,53] suggesting that WHA might be suitable for long-term volume stability at the regenerated sites.

The main strength of the study lies in the extent of data collected, with regards to time, space, and treatment groups. Bone regeneration was evaluated over the course of 6 months, which is a relatively long period for an in vivo study. Another strength was the IOS methodology used to record the original defect area (ROI1) consistently and precisely between defects in different treatment groups. This registration was particularly important to overcome limitations imposed by the collapsing of membranes in Sh + M group and the collapse of the soft tissue in Sh group. The IOS methodology was able to precisely define the actual physical surface of the mandible prior to and after creation of the defects and based upon the measurements done during histologic processing to determine the precise location of the slide area within the defect.[54] To our knowledge this is the first study using this volumetric methodology contributing for the precision of the histomorphometric results. In addition, the study was designed to include three control groups: one positive control treated with BO + M, and two negative controls (with or without a resorbable membrane) and for each defect, three histological slides were analyzed for histomorphometry. These characteristics allowed a more comprehensive view of the bone regeneration induced by the study materials.

The present study presents some limitations. It should be emphasized that the collection of the central and two lateral histological slides, due to technical limitations, was not always possible. However, the likelihood of any bias arising from this limitation is low, since it occurred in all treatment groups. Another limitation is related to the

FIGURE 10 High magnification histological samples of both WHA and BO groups in the different cohorts, corresponding to the red squares areas illustrated in Figure 9. At 4 weeks it is possible to observe that WHA presents a more osteoconductive behavior in between particles when compared to BO. At 12 and 26 weeks both biomaterials presents a similar osteoconductive behavior in between particles.
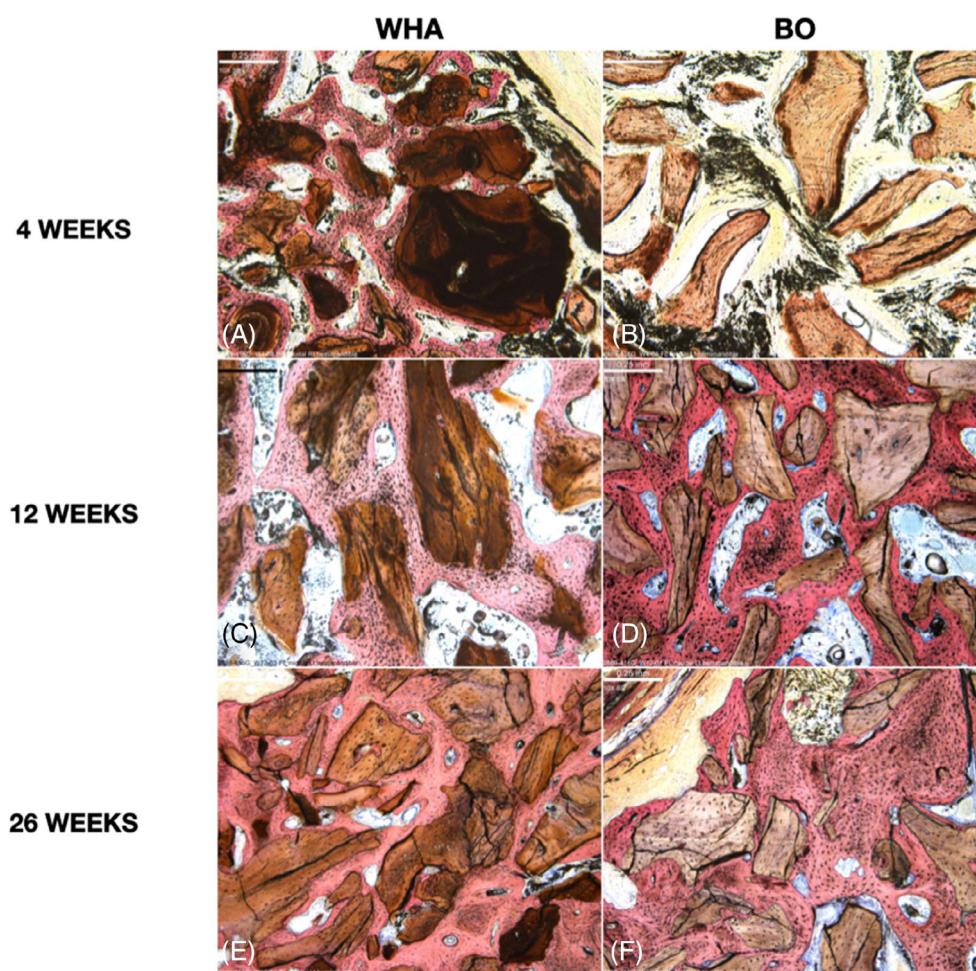
absence of immunohistochemical analysis. This could provide information about the bone regeneration cellular mechanism in both tested materials, providing broader information about the variations observed at 4 weeks with WHA + M and BO + M.

5 | CONCLUSIONS

WHA and BO resulted in similar at 12 and 26 weeks, with higher regenerative performance when compared to the sham controls. However, at 4 weeks, the defect regeneration was significantly enhanced by WHA compared to all other treatments. WHA showed excellent safety and biocompatibility at all three timepoints, which was comparable to that of BO.

AUTHOR CONTRIBUTIONS

Emilie Dory, Caroline Trus, Geoffrey Lecloux, France Lambert, and Eric Rompen designed the study; Geoffrey Lecloux, Bruno De Carvalho, and Eric Rompen carried out the study interventions and partially collected the data; Loïc Germain and Caroline Trus analyzed the data results outsourced; Bruno De Carvalho led the writing. All authors critically revised the manuscript and have given their approval for the final version to be published.

CONFLICT OF INTEREST STATEMENT

This study was funded by Wishbone SA. E.D., J.P. and C.T. are currently employees of Wishbone SA. L.G. was an employee of Wishbone SA during the study. F.L., G.L. and E.R. are founders and shareholders of Wishbone SA, and E.R. is a founder and shareholder of Wishbone Cy; their contribution to the study was limited and neither of them were involved in the analysis and interpretation of the results. For the histological processing and performance analyses, this

study was outsourced in GLP conditions. B.D.C. declares no competing interests.

DATA AVAILABILITY STATEMENT

The data that support the findings of this study are available from the corresponding author upon reasonable request.

ORCID

Bruno De Carvalho https://orcid.org/0000-0001-9527-7616

REFERENCES

1. Elani HW, Starr JR, Da Silva JD, Gallucci GO. Trends in dental implant use in the U.S., 1999–2016, and projections to 2026. *J Dent Res*. 2018;97(13):1424-1430. doi:10.1177/0022034518792567
2. Aghaloo TL, Moy PK. Which hard tissue augmentation techniques are the most successful in furnishing bony support for implant placement? *Int J Oral Maxillofac Implants*. 2007;22(suppl):49-70.
3. Esposito M, Grusovin MG, Rees J, et al. Interventions for replacing missing teeth: augmentation procedures of the maxillary sinus. *Cochrane Database Syst Rev*. 2010;3:CD008397. doi:10.1002/14651858.Cd008397
4. Jensen SS, Terheyden H. Bone augmentation procedures in localized defects in the alveolar ridge: clinical results with different bone grafts and bone-substitute materials. *Int J Oral Maxillofac Implants*. 2009;24-(suppl):218-236.
5. Jepsen S, Schwarz F, Cordaro L, et al. Regeneration of alveolar ridge defects. Consensus report of group 4 of the 15th European workshop on periodontology on bone regeneration. *J Clin Periodontol*. 2019;46-(suppl 21):277-286. doi:10.1111/jcpe.13121
6. Naenni N, Lim HC, Papageorgiou SN, Hämmerle CHF. Efficacy of lateral bone augmentation prior to implant placement: a systematic review and meta-analysis. *J Clin Periodontol*. 2019;46(suppl 21):287-306. doi:10.1111/jcpe.13052
7. Sanz-Sánchez I, Ortiz-Vigón A, Sanz-Martín I, Figuero E, Sanz M. Effectiveness of lateral bone augmentation on the alveolar crest dimension: a systematic review and meta-analysis. *J Dent Res*. 2015;94(9 suppl):128s-142s. doi:10.1177/0022034515594780
8. Chappuis V, Rahman L, Buser R, Janner SFM, Belser UC, Buser D. Effectiveness of contour augmentation with guided bone regeneration: 10-year results. *J Dent Res*. 2018;97(3):266-274. doi:10.1177/0022034517737755
9. Chiapasco M, Abati S, Romeo E, Vogel G. Clinical outcome of autogenous bone blocks or guided bone regeneration with e-PTFE membranes for the reconstruction of narrow edentulous ridges. *Clin Oral Implants Res*. 1999;10(4):278-288. doi:10.1034/j.1600-0501.1999.100404.x
10. Reynolds MA, Aichelmann-Reidy ME, Branch-Mays GL. Regeneration of periodontal tissue: bone replacement grafts. *Dent Clin N Am*. 2010;54(1):55-71. doi:10.1016/j.cden.2009.09.003
11. Shamsoddin E, Houshmand B, Golabgiran M. Biomaterial selection for bone augmentation in implant dentistry: a systematic review. *J Adv Pharm Technol Res*. 2019;10(2):46-50. doi:10.4103/japtr.JAPTR_327_18
12. Dasmah A, Thor A, Ekestubbe A, Sennerby L, Rasmusson L. Particulate vs. block bone grafts: three-dimensional changes in graft volume after reconstruction of the atrophic maxilla, a 2-year radiographic follow-up. *J Craniomaxillofac Surg*. 2012;40(8):654-659. doi:10.1016/j.jcms.2011.10.032
13. Esposito M, Felice P, Worthington HV. Interventions for replacing missing teeth: augmentation procedures of the maxillary sinus. *Cochrane Database Syst Rev*. 2014;5:CD008397. doi:10.1002/14651858.CD008397.pub2
14. Hallman M, Thor A. Bone substitutes and growth factors as an alternative/complement to autogenous bone for grafting in implant dentistry. *Periodontol 2000*. 2008;2000(47):172-192. doi:10.1111/j.1600-0757.2008.00251.x
15. Lambert F, Bacevic M, Layrolle P, Schüpbach P, Drion P, Rompen E. Impact of biomaterial microtopography on bone regeneration: comparison of three hydroxyapatites. *Clin Oral Implants Res*. 2017;28(10):e201-e207. doi:10.1111/clr.12986
16. Kolk A, Handschel J, Drescher W, et al. Current trends and future perspectives of bone substitute materials – from space holders to innovative biomaterials. *J Craniomaxillofac Surg*. 2012;40(8):706-718. doi:10.1016/j.jcms.2012.01.002
17. Trajkovski B, Jaunich M, Müller WD, Beuer F, Zafiropoulos GG, Houshmand A. Hydrophilicity, viscoelastic, and physicochemical properties variations in dental bone grafting substitutes. *Materials (Basel)*. 2018;11(2):215. doi:10.3390/ma11020215
18. Berberi A, Samarani A, Nader N, et al. Physicochemical characteristics of bone substitutes used in oral surgery in comparison to autogenous bone. *Biomed Res Int*. 2014;2014:320790. doi:10.1155/2014/320790
19. Al-Sanabani JS, Madfa AA, Al-Sanabani FA. Application of calcium phosphate materials in dentistry. *Int J Biomater*. 2013;2013:876132. doi:10.1155/2013/876132
20. Epple M, Ganesan K, Heumann R, et al. Application of calcium phosphate nanoparticles in biomedicine. *J Mater Chem*. 2010;20(1):18-23. doi:10.1039/B910885H
21. Filippi M, Born G, Chaaban M, Scherberich A. Natural polymeric scaffolds in bone regeneration. *Front Bioeng Biotechnol*. 2020;8:474. doi:10.3389/fbioe.2020.00474
22. Gunduz O, Erkan EM, Daglilar S, Salman S, Agathopoulos S, Oktar FN. Composites of bovine hydroxyapatite (BHA) and ZnO. *J Mater Sci*. 2008;43(8):2536-2540. doi:10.1007/s10853-008-2497-1
23. Sanz M, Dahlin C, Apatzidou D, et al. Biomaterials and regenerative technologies used in bone regeneration in the craniomaxillofacial region: consensus report of group 2 of the 15th European workshop on periodontology on bone regeneration. *J Clin Periodontol*. 2019;46-(suppl 21):82-91. doi:10.1111/jcpe.13123
24. De Carvalho B, Rompen E, Lecloux G, et al. Effect of sintering on in vivo biological performance of chemically deproteinized bovine hydroxyapatite. *Materials (Basel)*. 2019;12(23):3946. doi:10.3390/ma12233946
25. Lambert F, Léonard A, Drion P, Sourice S, Layrolle P, Rompen E. Influence of space-filling materials in subantral bone augmentation: blood clot vs. autogenous bone chips vs. bovine hydroxyapatite. *Clin Oral Implants Res*. 2011;22(5):538-545. doi:10.1111/j.1600-0501.2010.02069.x
26. Baldini N, De Sanctis M, Ferrari M. Deproteinized bovine bone in periodontal and implant surgery. *Dent Mater*. 2011;27(1):61-70. doi:10.1016/j.dental.2010.10.017
27. US FDA. Wishbone HA marketing authorization approval. 2021. https://www.accessdata.fda.gov/cdrh_docs/pdf21/K211551.pdf
28. Rompen E, Lambert F, Lecloux G, Moniotte P. Materiau de regeneration osseuse et son procede de fabrication. Patent WO 2015/049336 A1(12). 2015.
29. US FDA. GEISTLICH BIO-OSS®. 510(k) Summary. 2013. https://www.accessdata.fda.gov/cdrh_docs/pdf12/k122894.pdf
30. Aerssens J, Boonen S, Lowet G, Dequeker J. Interspecies differences in bone composition, density, and quality: potential implications for in vivo bone research. *Endocrinology*. 1998;139(2):663-670. doi:10.1210/endo.139.2.5751
31. International Organization for Standardization. ISO 10993-6:2016 (en). Biological evaluation of medical devices—Part 6: Tests for local effects after implantation. 2016. https://www.iso.org/obp/ui#iso:std:iso:10993:-6:ed-3:v1:en

32. Faul F, Erdfelder E, Lang A-G, Buchner A. G*Power 3: a flexible statistical power analysis program for the social, behavioral, and biomedical sciences. *Behav Res Methods*. 2007;39(2):175-191. doi:10.3758/bf03193146

33. Weibrich G, Trettin R, Gnoth SH, Götz H, Duschner H, Wagner W. Determining the size of the specific surface of bone substitutes with gas adsorption. *Mund Kiefer Gesichtschir*. 2000;4(3):148-152. doi:10.1007/s100060050187

34. Bohner M. Calcium orthophosphates in medicine: from ceramics to calcium phosphate cements. *Injury*. 2000;31(suppl 4):37-47. doi:10.1016/s0020-1383(00)80022-4

35. Habibovic P, Kruyt MC, Juhl MV, et al. Comparative in vivo study of six hydroxyapatite-based bone graft substitutes. *J Orthop Res*. 2008;26(10):1363-1370. doi:10.1002/jor.20648

36. Patel N, Gibson IR, Ke S, Best SM, Bonfield W. Calcining influence on the powder properties of hydroxyapatite. *J Mater Sci Mater Med*. 2001;12(2):181-188. doi:10.1023/a:1008986430940

37. Aquino-Martínez R, Artigas N, Gámez B, Rosa JL, Ventura F. Extracellular calcium promotes bone formation from bone marrow mesenchymal stem cells by amplifying the effects of BMP-2 on SMAD signalling. *PLoS One*. 2017;12(5):e0178158. doi:10.1371/journal.pone.0178158

38. Kwon S-H, Jun Y-K, Hong S-H, Lee I-S, Kim H-E, Won YY. Calcium phosphate bioceramics with various porosities and dissolution rates. *J Am Ceram Soc*. 2002;85(12):3129-3131. doi:10.1111/j.1151-2916.2002.tb00599.x

39. Araújo M, Linder E, Lindhe J. Effect of a xenograft on early bone formation in extraction sockets: an experimental study in dog. *Clin Oral Implants Res*. 2009;20(1):1-6. doi:10.1111/j.1600-0501.2008.01606.x

40. Cardaropoli G, Araújo M, Hayacibara R, Sukekava F, Lindhe J. Healing of extraction sockets and surgically produced – augmented and non-augmented – defects in the alveolar ridge. An experimental study in the dog. *J Clin Periodontol*. 2005;32(5):435-440. doi:10.1111/j.1600-051X.2005.00692.x

41. Liu Q, Huang S, Matinlinna JP, Chen Z, Pan H. Insight into biological apatite: physiochemical properties and preparation approaches. *Biomed Res Int*. 2013;2013:929748. doi:10.1155/2013/929748

42. Lambert F, Leonard A, Lecloux G, Sourice S, Pilet P, Rompen E. A comparison of three calcium phosphate-based space fillers in sinus elevation: a study in rabbits. *Int J Oral Maxillofac Implants*. 2013;28(2):393-402. doi:10.11607/jomi.2332

43. Molly L, Vandromme H, Quirynen M, Schepers E, Adams JL, van Steenberghe D. Bone formation following implantation of bone biomaterials into extraction sites. *J Periodontol*. 2008;79(6):1108-1115. doi:10.1902/jop.2008.070476

44. Dimitriou R, Mataliotakis GI, Calori GM, Giannoudis PV. The role of barrier membranes for guided bone regeneration and restoration of large bone defects: current experimental and clinical evidence. *BMC Med*. 2012;10:81. doi:10.1186/1741-7015-10-81

45. Friedmann A, Gissel K, Soudan M, Kleber BM, Pitaru S, Dietrich T. Randomized controlled trial on lateral augmentation using two collagen membranes: morphometric results on mineralized tissue compound. *J Clin Periodontol*. 2011;38(7):677-685. doi:10.1111/j.1600-051X.2011.01738.x

46. Merli M, Moscatelli M, Mariotti G, Pagliaro U, Raffaelli E, Nieri M. Comparing membranes and bone substitutes in a one-stage procedure for horizontal bone augmentation. Three-year post-loading results of a double-blind randomised controlled trial. *Eur J Oral Implantol*. 2018;11(4):441-452.

47. Aprile P, Letourneur D, Simon-Yarza T. Membranes for guided bone regeneration: a road from bench to bedside. *Adv Healthc Mater*. 2020;9(19):e2000707. doi:10.1002/adhm.202000707

48. Retzepi M, Donos N. Guided bone regeneration: biological principle and therapeutic applications. *Clin Oral Implants Res*. 2010;21(6):567-576. doi:10.1111/j.1600-0501.2010.01922.x

49. Elnayef B, Porta C, Suárez-López Del Amo F, Mordini L, Gargallo-Albiol J, Hernández-Alfaro F. The fate of lateral ridge augmentation: a systematic review and meta-analysis. *Int J Oral Maxillofac Implants*. 2018;33(3):622-635. doi:10.11607/jomi.6290

50. Chiba S, Anada T, Suzuki K, et al. Effect of resorption rate and osteoconductivity of biodegradable calcium phosphate materials on the acquisition of natural bone strength in the repaired bone. *J Biomed Mater Res A*. 2016;104(11):2833-2842. doi:10.1002/jbm.a.35828

51. Hannink G, Arts JJ. Bioresorbability, porosity and mechanical strength of bone substitutes: what is optimal for bone regeneration? *Injury*. 2011;42(suppl 2):S22-S25. doi:10.1016/j.injury.2011.06.008

52. Wach T, Kozakiewicz M. Fast-versus slow-resorbable calcium phosphate bone substitute materials-texture analysis after 12 months of observation. *Materials (Basel)*. 2020;13(17):3854. doi:10.3390/ma13173854

53. Kim YJ, Saiki CET, Silva K, et al. Bone formation in grafts with Bio-Oss and autogenous bone at different proportions in rabbit Calvaria. *Int J Dent*. 2020;2020:2494128. doi:10.1155/2020/2494128

54. Lo Russo L, Caradonna G, Troiano G, Salamini A, Guida L, Ciavarella D. Three-dimensional differences between intraoral scans and conventional impressions of edentulous jaws: a clinical study. *J Prosthet Dent*. 2020;123(2):264-268. doi:10.1016/j.prosdent.2019.04.004

APPENDIX A

Table A1

TABLE A1 Histologic evaluation system for cell type/tissue response.

Response	Score				
	0	1	2	3	4
Polymorphonuclear cells	Absent	Rare, 1–5/hpf	6–10/hpf	Heavy infiltrate	Packed
Lymphocytes	Absent	Rare, 1–5/hpf	6–10/hpf	Heavy infiltrate	Packed
Plasma cells	Absent	Rare, 1–5/hpf	6–10/hpf	Heavy infiltrate	Packed
Macrophages	Absent	Rare, 1–5/hpf	6–10/hpf	Heavy infiltrate	Packed
Giant cells	Absent	Rare, 1–2/hpf	3–5/hpf	Heavy infiltrate	Packed
Necrosis	Absent	Minimal	Mild	Moderate	Marked
Fibrinous exudates	Absent	Minimal	Mild	Moderate	Marked
Tissue degeneration	Absent	Minimal	Mild	Moderate	Marked
Neovascularization	Absent	Minimal capillary proliferation, focal, 1–3 buds	Groups of 4–7 capillaries with supporting fibroblastic structures	Broad band of capillaries with supporting structures	Extensive band of capillaries with supporting fibroblastic structures
Fibrocytes/ fibroconnective tissue, fibrosis	Absent	Narrow band	Moderately thick band	Thick band	Extensive band
Fatty infiltrate	Absent	Minimal amount of fat associated with fibrosis	Several layers of fat and fibrosis	Elongated and broad accumulation of fat cells around the implant site	Extensive fat completely surrounding the implant

Note: Minimal: observation was barely perceptible microscopically and was not believed to have clinical significance; Mild: observation was visible but involved a minor proportion of the tissue, and the clinical consequences of the observation were most likely subclinical; Moderate: observation was clearly visible and involved a significant proportion of the tissue; it was likely to have some clinical manifestations, but which were generally expected to be minor; Marked: observation was clearly visible and involved a major proportion of the tissue; clinical manifestations were probable and may have been associated with significant tissue.

Abbreviation: hpf, high powered (400×) field.